IEEE Photonics Journal
An IEEE Photonics Society Publication

Open Access

Two-Way Mixed RF/FSO Relaying System in the Presence of Co-channel Interference

Volume 11, Number 2, April 2019

Zhuo Wang
Wenxiao Shi
Wei Liu

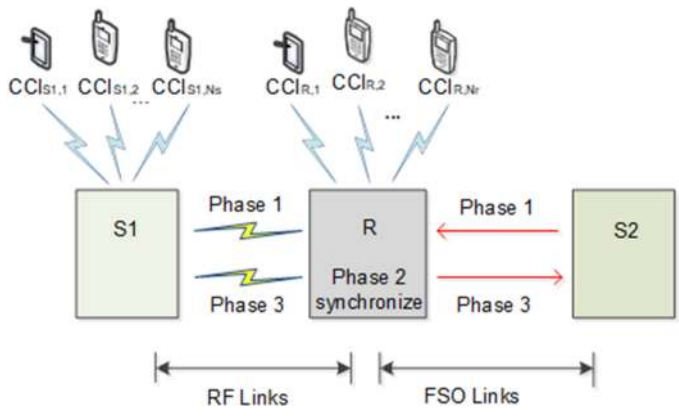

DOI: 10.1109/JPHOT.2019.2904521
1943-0655 © 2019 IEEE

IEEE photonics SOCIETY

IEEE

Two-Way Mixed RF/FSO Relaying System in the Presence of Co-channel Interference

Zhuo Wang, Wenxiao Shi, and Wei Liu

College of Communication Engineering, Jilin University, Changchun 130012, P.R. China

DOI:10.1109/JPHOT.2019.2904521

Manuscript received January 29, 2019; revised March 1, 2019; accepted March 6, 2019. Date of publication March 22, 2019; date of current version April 1, 2019. This work was supported by the National Natural Science Foundation of China under Grant 61373124 and Grant 61601195. Corresponding author: Wenxiao Shi (e-mail. swx@jlu.edu.cn).

Abstract: In this paper, the performance of a two-way mixed radio frequency/free space optical (RF/FSO) relaying system in the presence of co-channel interference (CCI) is investigated. The RF links are modeled as Nakagami-m distribution, and FSO links adopt Gamma-Gamma turbulence model. To improve spectral efficiency, relay exchanges the information between two terminals in three phases via RF and FSO links. Meanwhile, CCIs are considered at both relay and destination. Novel closed-form upper bounds expressions for the signal to interference plus noise ratios are derived, based on that lower bounds outage probability, average bit error rate, and outage capacity are further presented for both RF/FSO and FSO/RF links. Then, asymptotic expressions are provided to predict the diversity order. Additionally, the effect of various parameters on system performance, such as interference numbers and power, are investigated and compared including interference-free condition. Simulation results show that, in the interference-effected system, when the average signal-to-noise ratio increases, system performance enhances first and then remains unchanged. This phenomenon does not occur in the interference-free system, which implies the system performance is limited by the numbers and power of CCIs. Moreover, the effect of pointing errors on system performance is further investigated.

Index Terms: Mixed RF/FSO, two-way relaying, co-channel interference, outage probability.

1. Introduction

As one of the most promising technologies for future wireless communication, cooperative diversity schemes can make full use of network resources to achieve high data rate and high reliability communication [1]. Initially, the concept of cooperative strategy comes from radio frequency (RF) communication. Later on, there is an extension use in free space optical (FSO) system, which receives considerable attention. Different cooperative strategies have been investigated in FSO system, including relay-assisted and multiple-inputs multiple-outputs technologies, etc. [2]. Among them, relay-assisted technology combines the advantages of RF and FSO links, an asymmetric dual-hop mixed RF/FSO relaying system is formed. Compared with traditional RF/RF communication, a mixed RF/FSO system can enhance data rate and capacity significantly [3]. Most importantly, since RF and FSO links operate on different frequency bands, the interference between two links is avoided.

How to improve spectral efficiency (SE) has always been a hot issue in the field of wireless communication. In a one-way single relay system, the information exchanges between two nodes

generally need three or four phases [3]. However, in a two-way system, only two phases are required. In the first phase, two nodes send the information to the relay, and then the relay exchanges the information to the destination in the second phase. In this way, SE is improved dramatically. The authors in [4] investigated the performance of a two-way multiuser mixed RF/FSO system, outage probability (OP) and average ergodic channel capacity were studied and simulated, opportunistic user scheduling and asymmetric channel fading were considered respectively. Later, they derived the average symbol error rate in the similar configure [3], optimal transmission power allocation was discussed using asymptotic results. In order to solve the synchronization issue caused by different data rates of RF and FSO, a three phases bidirectional mixed RF/FSO system was proposed in [5], OP and bit error rate (BER) expressions were presented. A novel network-coded two-way mixed FSO/RF system was considered in [6], the best relay location was obtained for the system. In [7], a half-duplex two-way relay mixed RF/FSO system was investigated, OP and BER were calculated, asymptotic behavior and diversity orders were analyzed at high signal to noise ratio (SNR). Inspired by [5], a three phases two-way mixed RF/FSO system in the presence of co-channel interference (CCI) is investigated in this paper.

On the other hand, as a dominant factor caused by frequency reuse, CCI was also considered in mixed RF/FSO system. In [8], the authors examined the OP performance of mixed RF/FSO system with relay corrupted by CCI. Later, they extended their work to multiple CCIs in [9], where the RF links followed Nakagami-m distribution and pointing errors were taken into account in FSO links. Multiple CCIs were considered at both relay and destination in [10], where OP and BER expressions of mixed RF/FSO system with an extra direct link were derived. Besides OP and BER, ergodic capacity performance of the system with multiple CCIs was simulated in [11]. More recently, a multiuser mixed RF/FSO system with CCI under eavesdropping attack was analyzed in [12], OP performance was derived with Nakagami-m/Gamma–Gamma fading models, secrecy performance and power allocation optimization problem were also investigated particularly. While all these previous works improved our understanding of mixed RF/FSO relaying system, we find that most of the literatures studied the effect of CCIs in a one-way system, the performance of a two-way mixed RF/FSO relaying system with CCIs has not been investigated yet. Moreover, since both relay and destination receive RF signals in the two-way system, CCIs should be considered simultaneously.

Motivated by the works above, we propose a two-way mixed RF/FSO relaying system with CCIs considering at all the nodes which receive RF signals. As far as we know, this system has not been proposed or investigated yet. Therefore, we derive the tight lower bounds OP, BER and outage capacity of this interference-effected two-way mixed RF/FSO system. Additionally, asymptotic expressions of OP are calculated in order to further analyze the impact of various parameters on system performance. The main contributions of this paper can be summarized as follows

1) An interference-effected two-way mixed RF/FSO system is proposed, where multiple CCIs are considered at both relay and destination. This configuration can better reflect practical scenes and has not been received enough attention yet. Additionally, to solve the synchronization issue between RF and FSO links, a three phases two-way relaying scheme is adopted in this paper.
2) Novel closed-form upper bounds expressions for signal to interference plus noise ratios (SINRs) are derived. Based on that lower bounds OP, average BER and outage capacity are further presented for both RF/FSO and FSO/RF links. Moreover, asymptotic expressions of OP are given, which can provide a simple method to predict the diversity order of the system.
3) The effect of various parameters on system performance is studied such as interference numbers and power, in particular, no interference condition is compared. Pointing errors are also taken into account.

The rest of this paper is organized as follows. Section 2 presents system and channel models. Statistical analyses of end-to-end SINRs are presented in Section 3. Tight closed-form lower bounds and asymptotic expressions of OP are derived in Section 4. BER and outage capacity expressions

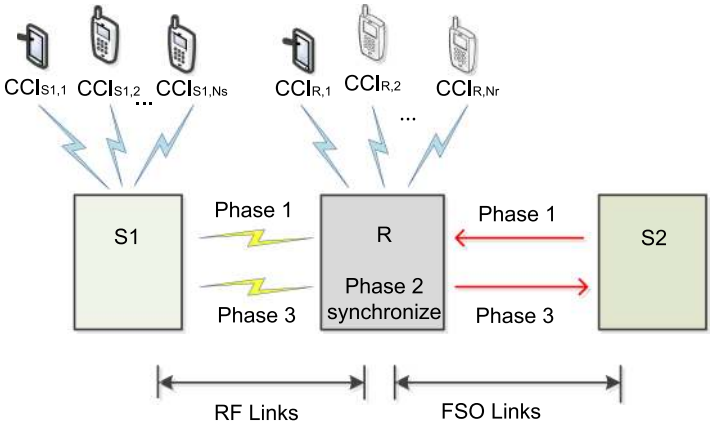

Fig. 1. A two-way mixed RF/FSO relaying system with CCIs.

are provided in Section 5. Simulations and numerical results are investigated in Section 6. Finally, Section 7 concludes the paper.

2. System and Channel Models

As illustrated in Fig. 1, we consider a two-way mixed RF/FSO relaying system consisted of two end nodes (S1 and S2) and a relay node R. End nodes are equipped with a single transmitter and receiver, while relay node is deployed by two pairs of transceivers. End nodes exchange their information in three phases. In the first phase, S1 and S2 send the signals to R, while in the second phase, the relay synchronizes the signals, to make sure the received RF and FSO signals are processed simultaneously. Finally, the relay forwards the signals back to S1 and S2 in the third phase. Assume S1-R and S2-R are equipped with RF and FSO links, respectively, where the RF links are subjected to Nakagami-m distribution and FSO links follow Gamma-Gamma model with pointing errors. Moreover, we assume the interferers are located near the cell edge, the effect of CCIs from adjacent cells cannot be neglected. Thus, CCIs are considered at S1 and R when receiving RF signals, since S2 transmits and receives optical signals, there is no CCI at S2.

2.1 System Model

In this system, P_{S1}, P_{S2} and P_R represent the average transmitted power at S1, S2 and R. $P_{R,i}$ and $P_{S1,j}$ denote the *i*-th and *j*-th average transmitted power of CCIs at R and S1. Additionally, f and g are the channel coefficients between S1-R and S2-R, which is viceversa. $h_{R,i}$ and $h_{S1,j}$ are the channel coefficients of *i*-th and *j*-th CCIs at R and S1. *Nr* and *Ns* are the numbers of CCIs at R and S1.

The received signal at relay can be expressed as

$$y_R = \sqrt{P_{S1}} f x_{S1} + \eta_1 \sqrt{P_{S2}} g x_{S2} + \sum_{i=1}^{N_r} \sqrt{P_{R,i}} h_{R,i} x_{R,i} + n_R \tag{1}$$

where x_{S1} and x_{S2} are the transmit signals from $S1$ and $S2$, $x_{R,i}$ is the *i*-th interference signal at the relay, η_1 is the optical-to-electrical conversion coefficient, n_R is additive white Gaussian noise (AWGN) at the relay with power of σ^2.

The relay amplifies the received signal with variable gain G, taking CCIs and noise into account, the signal received at $S1$ can be given by

$$y_{S1} = \sqrt{P_R} G f y_R + \sum_{j=1}^{N_s} \sqrt{P_{S1,j}} h_{S1,j} x_{S1,j} + n_{S1} \tag{2}$$

where $x_{S1,j}$ is the j-th interference signal at $S1$, n_{S1} is AWGN at $S1$ with power of σ^2, since [13]

$$G^{-1} \triangleq \sqrt{P_{S1}|f|^2 + \eta_1^2 P_{S2}|g|^2 + \sum_{i=1}^{N_r} P_{R,i}\left|h_{R,i}\right|^2 + \sigma^2} \tag{3}$$

Assumed S_1 can eliminate the signal it sends, the received signal at S_1 can be presented as

$$y_{S1} = \sqrt{P_R}\sqrt{P_{S2}}\eta_1 Gfgx_{S2} + \sqrt{P_R}Gf\sum_{i=1}^{N_r}\sqrt{P_{R,i}}h_{R,i}x_{R,i} + \sum_{j=1}^{N_s}\sqrt{P_{S1,j}}h_{S1,j}x_{S1,j} + \sqrt{P_R}Gfn_R + n_{S1} \tag{4}$$

Then, the SINR at $S1$ can be derived as

$$\gamma_{SINR}^{S1} = \frac{P_R P_{S2}\eta_1^2 G^2|f|^2|g|^2}{P_R G^2|f|^2\sum_{i=1}^{N_r} P_{R,i}\left|h_{R,i}\right|^2 + \sum_{j=1}^{N_s} P_{S1,j}\left|h_{S1,j}\right|^2 + P_R G^2|f|^2\sigma^2 + \sigma^2} \tag{5}$$

Bring into G in Eq. (3), after some mathematical simplification, the result can be

$$\gamma_{SINR}^{S1} = \frac{\dfrac{P_R P_{S2}\eta_1^2|f|^2|g|^2}{\left(\sum_{i=1}^{N_r} P_{R,i}\left|h_{R,i}\right|^2 + \sigma^2\right)\left(\sum_{j=1}^{N_s} P_{S1,j}\left|h_{S1,j}\right|^2 + \sigma^2\right)}}{\dfrac{P_R|f|^2}{\left(\sum_{j=1}^{N_s} P_{S1,j}\left|h_{S1,j}\right|^2 + \sigma^2\right)} + \dfrac{\left(P_{S1}|f|^2 + P_{S2}\eta_1^2|g|^2\right)}{\left(\sum_{i=1}^{N_r} P_{R,i}\left|h_{R,i}\right|^2 + \sigma^2\right)} + 1} \tag{6}$$

Assume $\rho \triangleq P_R/P_{S1}$, the instantaneous SNRs for $S1$-R and $S2$-R are defined as $\gamma_1 = P_{S1}|f|^2/\sigma^2$, $\gamma_2 = \eta_1^2 P_{S2}|g|^2/\sigma^2$, the instantaneous interference-to-noise ratios for $S1$ and R are defined as $\gamma_S = \gamma_S' + 1 = \sum_{j=1}^{N_s}\gamma_{S1,j} + 1 = \sum_{j=1}^{N_s} P_{S1,j}|h_{S1,j}|^2/\sigma^2 + 1$, $\gamma_R = \gamma_R' + 1 = \sum_{i=1}^{N_r}\gamma_{R,i} + 1 = \sum_{i=1}^{N_r} P_{R,i}|h_{R,i}|^2/\sigma^2 + 1$. Thus, the SINR at $S1$ can be simplified to

$$\gamma_{SINR}^{S1} = \frac{\rho\dfrac{\gamma_1\gamma_2}{\gamma_S\gamma_R}}{\rho\dfrac{\gamma_1}{\gamma_S} + \dfrac{\gamma_1 + \gamma_2}{\gamma_R} + 1} \tag{7}$$

To simplify calculation, the tightly upper bounds of SINR is derived as

$$\gamma_{SINR}^{S1} \le \frac{\rho\dfrac{\gamma_1\gamma_2}{\gamma_S\gamma_R}}{\rho\dfrac{\gamma_1}{\gamma_S} + \dfrac{\gamma_1 + \gamma_2}{\gamma_R}} = \frac{\rho\dfrac{\gamma_1\gamma_2}{\gamma_S(\gamma_S + \rho\gamma_R)}}{\dfrac{\gamma_1}{\gamma_S} + \dfrac{\gamma_2}{(\gamma_S + \rho\gamma_R)}} \le \rho min\left(\frac{\gamma_1}{\gamma_S}, \frac{\gamma_2}{\gamma_S + \rho\gamma_R}\right) \tag{8}$$

Likewise, the received signal at S2 after amplified by variable gain relay can be denoted as

$$y_{S2} = \eta_2 Gg\sqrt{P_R}y_R + n_{S2} \tag{9}$$

where η_2 is the electrical-to-optical conversion coefficient, n_{S2} is AWGN at $S2$ with power of σ^2.

After removing the signal sent by S2, the SINR at S2 can be

$$\gamma_{SINR}^{S2} = \frac{\eta_2^2 G^2|g|^2 P_{S1}P_R|f|^2}{\eta_2^2 G^2|g|^2 P_R\sum_{i=1}^{N_r} P_{R,i}\left|h_{R,i}\right|^2 + \eta_2^2 G^2|g|^2 P_R\sigma^2 + \sigma^2} \tag{10}$$

Assumed $\mu \triangleq P_R/P_{S2}$, $\kappa \triangleq \eta_1^2/\eta_2^2$, after some mathematical derivations similar to above, upper bounds SINR at S2 can be obtained as

$$\gamma_{SINR}^{S2} \le \frac{\kappa\mu\dfrac{\gamma_1\gamma_2}{\gamma_R}}{\kappa\mu\gamma_2 + \dfrac{\gamma_1 + \gamma_2}{\gamma_R}} = \frac{\kappa\mu\gamma_1\gamma_2}{\gamma_2(\kappa\mu\gamma_R + 1) + \gamma_1} \le \kappa\mu min\left(\gamma_2, \frac{\gamma_1}{\kappa\mu\gamma_R + 1}\right) \tag{11}$$

2.2 Channel Model

As previously mentioned, the RF links for S1-R and CCIs are subjected to Nakagami-m distribution, FSO links for S2-R follow Gamma-Gamma model with pointing errors.

If f is subjected to Nakagami-m distribution, the SNR $\gamma_1 = P_{S1}|f|^2/\sigma^2$ are Gamma random variables (RVs) with two parameters, m is the shape parameter which represents fading severity ($m \geq 0.5$), Ω/m is the scale parameter, where Ω denotes the mean value of Gamma RVs [13]. Thus, the distributions can be obtained as

$$\gamma_1 \sim G(m_1, \overline{\gamma_1}/a)\ \gamma_{S1,j} \sim G(m_s, 1/\alpha)\ \gamma_{R,i} \sim G(m_r, 1/\beta) \tag{12}$$

where $a \triangleq \frac{m_1}{\Omega_1}$, $\overline{\gamma_1} = \frac{P_{S1}}{\sigma^2}$, $\alpha \triangleq \frac{m_s\sigma^2}{\Omega_s P_{S1,j}}$, $\beta \triangleq \frac{m_r\sigma^2}{\Omega_r P_{R,i}}$. G (a, b) denotes the Gamma distribution.

Because of the additivity of i.i.d. Gamma RVs, the distribution of γ_S' and γ_R' can be obtained as

$$\gamma_S' \sim G(N_s m_s, 1/\alpha)\ \ \gamma_R' \sim G(N_r m_r, 1/\beta) \tag{13}$$

The PDF and CDF of Gamma RVs $G(a, b)$ are expressed as [13]

$$f_\gamma(\gamma) = \frac{\gamma^{a-1}}{b^a \Gamma(a)} \exp\left(-\frac{\gamma}{b}\right) \tag{14}$$

$$F_\gamma(\gamma) = 1 - \frac{\Gamma\left(a, \frac{\gamma}{b}\right)}{\Gamma(a)} \tag{15}$$

For Gamma-Gamma turbulence model, the PDF of instantaneous SNR with pointing errors can be given as [14]

$$f(\gamma_{FSO}) = \frac{\varphi^2}{2\Gamma(p)\Gamma(q)\gamma_{FSO}} G_{1,3}^{3,0}\left[\zeta p q \sqrt{\frac{\gamma_{FSO}}{\overline{\gamma_2}}} \,\middle|\, \begin{matrix} \varphi^2+1 \\ \varphi^2, p, q \end{matrix}\right] \tag{16}$$

where $\Gamma(.)$ is Gamma function, p and q are the fading parameters related to atmospheric turbulence, the higher values of p and q indicates the smaller impact of turbulence. φ is the pointing error parameter which denotes the ratio between the equivalent beam radius and the pointing error displacement standard deviation at the receiver [14], $\zeta = \frac{\varphi^2}{\varphi^2+1}$.

The CDF of instantaneous SNR can be obtained by [14]

$$F(\gamma_{FSO}) = \frac{2^{p+q-2}\varphi^2}{2\pi\Gamma(p)\Gamma(q)} G_{3,7}^{6,1}\left[\frac{(pq\zeta)^2\gamma_{FSO}}{16\overline{\gamma_2}} \,\middle|\, \begin{matrix} 1, \frac{\varphi^2+1}{2}, \frac{\varphi^2+2}{2} \\ \frac{\varphi^2}{2}, \frac{\varphi^2+1}{2}, \frac{p}{2}, \frac{p+1}{2}, \frac{q}{2}, \frac{q+1}{2}, 0 \end{matrix}\right] \tag{17}$$

3 Statistical Analysis

The upper bounds SINR at S1 and S2 are derived in Eq. (8) and Eq. (11), respectively. In order to derive the CDF of γ_{SINR}^{S1} and γ_{SINR}^{S2}, the CDFs of $\frac{\gamma_1}{\gamma_S}$, $\frac{\gamma_2}{\gamma_S+\rho\gamma_R}$, γ_2, $\frac{\gamma_1}{\kappa\mu\gamma_R+1}$ need to be computed first.

Proposition 1

Derivation process for the CDF of γ_1/γ_S is shown as follows

$$\begin{aligned} F\left(\frac{\gamma_1}{\gamma_S} < z\right) &= F(\gamma_1 < z\gamma_S) \\ &= \int_0^\infty F(\gamma_1 < z\gamma_S|\gamma_S) f(\gamma_S)\, d\gamma_S \end{aligned} \tag{18}$$

Since the PDF of γ_S' can be obtained from Eq. (13), it is easy to conduct the PDF of γ_S and γ_R as

$$f(\gamma_S) = \frac{(\gamma_S - 1)^{N_S M_S - 1}(\alpha)^{N_S M_S}}{\Gamma(N_S M_S)} \exp(-\alpha(\gamma_S - 1)) \quad f(\gamma_R) = \frac{(\gamma_R - 1)^{N_r M_r - 1}(\beta)^{N_r M_r}}{\Gamma(N_r M_r)} \exp(-\beta(\gamma_R - 1)) \tag{19}$$

By substituting Eq. (12) and Eq. (19) into Eq. (18), for integer m_1 using [15, Eq. (8.352.2)], [15, Eq. (17.13.3)] and binomial coefficient expansion, the final result becomes

$$\begin{aligned} F\left(\frac{\gamma_1}{\gamma_S} < z\right) &= 1 - \frac{\alpha^{N_s m_s}}{\Gamma(m_1)\Gamma(N_s m_s)} \int_0^\infty \Gamma(m_1, a(x+1)z/\overline{\gamma_1}) x^{N_s m_s - 1} \exp(-\alpha x)\, dx \\ &= 1 - \frac{\alpha^{N_s m_s}}{\Gamma(N_s m_s)} \sum_{i=0}^{m_1 - 1} \sum_{j=0}^{i} (az/\overline{\gamma_1})^j \binom{i}{j} \frac{\exp(-az/\overline{\gamma_1})}{i!} \int_0^\infty x^{j + N_s m_s - 1} \exp(-(\alpha + az/\overline{\gamma_1})x)\, dx \\ &= 1 - \frac{\alpha^{N_s m_s}}{\Gamma(N_s m_s)} \sum_{i=0}^{m_1 - 1} \sum_{j=0}^{i} (az/\overline{\gamma_1})^j \binom{i}{j} \frac{\exp(-az/\overline{\gamma_1})}{i!} \frac{\Gamma(j + N_s m_s)}{(\alpha + az/\overline{\gamma_1})^{j + N_s m_s}} \end{aligned} \tag{20}$$

Proposition 2

Similar to the process above, the CDFs of $\frac{\gamma_1}{\kappa\mu\gamma_R + 1}$ can be computed in the same way, to simplify calculation final result is approximately given as

$$\begin{aligned} F\left(\frac{\gamma_1}{\kappa\mu\gamma_R + 1} < z\right) &= \int_0^\infty F(\gamma_1 < z(\kappa\mu\gamma_R + 1) | \gamma_R) f(\gamma_R)\, d\gamma_R \\ &\geq 1 - \frac{(\beta)^{N_r M_r}}{\Gamma(N_r M_r)} \exp\left(-(\kappa\mu + 1) a \frac{z}{\overline{\gamma_1}}\right) \sum_{l=0}^{m_1 - 1} \sum_{d=0}^{l} \binom{l}{d} \\ &\quad \times \frac{\left(a\frac{z}{\overline{\gamma_1}}\right)^l (\kappa\mu)^d}{l!} (\kappa\mu + 1)^{l-d} \Gamma(d + N_r M_r) \left(\beta + \frac{az}{\overline{\gamma_1}}\kappa\mu\right)^{-(d + N_r M_r)} \end{aligned} \tag{21}$$

Proposition 3

The CDF of $\frac{\gamma_2}{\gamma_S + \rho\gamma_R}$ is derived as follows

$$\begin{aligned} F\left(\frac{\gamma_2}{\gamma_S + \rho\gamma_R} < z\right) &= F\left(\frac{\gamma_S + \rho\gamma_R}{\gamma_2} > \frac{1}{z}\right) = 1 - F\left(\frac{\gamma_S + \rho\gamma_R}{\gamma_2} < \frac{1}{z}\right) \\ &= 1 - \int_0^\infty \Pr\left[(\gamma_S + \rho\gamma_R) < \frac{\gamma_2}{z} \middle| \gamma_2\right] f(\gamma_2)\, d\gamma_2 \end{aligned} \tag{22}$$

To compute the integral above, the CDF of $F(\gamma_S + \rho\gamma_R < z)$ need to be derived first as

$$F(\gamma_S + \rho\gamma_R < z) = F(\gamma_S < z - \rho\gamma_R) = \int_0^\infty \Pr[\gamma_S < z - \rho\gamma_R | \gamma_R] f(\gamma_R)\, d\gamma_R \tag{23}$$

The CDF of γ_S can be expressed as

$$F(\gamma_S < z) = F(\gamma_s' < z - 1) = 1 - \frac{\Gamma(N_s M_s, \alpha(z-1))}{\Gamma(N_s M_s)} \tag{24}$$

By substituting Eq. (19) and Eq. (24) into Eq. (23), $N_s M_s$ should also be integer, after some mathematical operations using [15, Eq. (8.352.2)], [15, Eq. (17.13.3)] and binomial coefficient

expansion, there is

$$F\left(\gamma_S+\rho\gamma_R<z\right)\geq 1-\frac{\beta^{N_rM_r}}{\Gamma\left(N_rM_r\right)}\exp\left(-\alpha\left(z-\rho-1\right)\right)\sum_{t=0}^{N_sM_s-1}\sum_{k=0}^{t}\binom{t}{k}\frac{\alpha^t(-\rho)^k}{t!}(z-\rho-1)^{t-k}$$

$$\int_0^\infty x^{k+N_rM_r-1}\exp\left(-\left(\beta-\alpha\rho\right)x\right)dx=1-\frac{\beta^{N_rM_r}}{\Gamma\left(N_rM_r\right)}\exp\left(-\alpha\left(z-\rho-1\right)\right)$$

$$\sum_{t=0}^{N_sM_s-1}\sum_{k=0}^{t}\binom{t}{k}\frac{\alpha^t(-\rho)^k}{t!}(z-\rho-1)^{t-k}\frac{\Gamma\left(k+N_rM_r\right)}{\left(\beta-\alpha\rho\right)^{k+N_rM_r}}\quad(\beta>\alpha\rho)\tag{25}$$

Substituting Eq. (25) into Eq. (22), there is

$$F\left(\frac{\gamma_S+\rho\gamma_R}{\gamma_2}<\frac{1}{z}\right)=\int_0^\infty \Pr\left[\left(\gamma_S+\rho\gamma_R\right)<\frac{\gamma_2}{z}\middle|\gamma_2\right]f\left(\gamma_2\right)d\gamma_2$$

$$=1-\frac{\varphi^2}{2\Gamma\left(p\right)\Gamma\left(q\right)}\frac{\beta^{N_rM_r}}{\Gamma\left(N_rM_r\right)}\exp\left(\left(\rho+1\right)\alpha\right)\sum_{t=0}^{N_sM_s-1}\sum_{k=0}^{t}\binom{t}{k}\frac{\alpha^t(-\rho)^k}{t!}\frac{\Gamma\left(k+N_rM_r\right)}{\left(\beta-\alpha\rho\right)^{k+N_rM_r}}$$

$$\times\int_0^\infty\exp\left(-\alpha\frac{\gamma_2}{z}\right)\left(\frac{\gamma_2}{z}-\rho-1\right)^{t-k}\gamma_2^{-1}G_{1,3}^{3,0}\left[\zeta pq\sqrt{\frac{\gamma_2}{\gamma_2}}\middle|\begin{matrix}\varphi^2+1\\ \varphi^2,p,q\end{matrix}\right]d\gamma_2\tag{26}$$

Using binomial coefficient expansion and [16, Eq. (07.34.21.0013.01)], final result is expressed as

$$F\left(\frac{\gamma_2}{\gamma_S+\rho\gamma_R}<z\right)=A\sum_{t=0}^{N_sM_s-1}\sum_{k=0}^{t}\sum_{n=0}^{t-k}\binom{t}{k}\binom{t-k}{n}\frac{\alpha^{t-n}(-\rho)^k}{t!}\frac{\Gamma\left(k+N_rM_r\right)}{\left(\beta-\alpha\rho\right)^{k+N_rM_r}}$$

$$\times(-\rho-1)^{t-k-n}G_{3,6}^{6,1}\left[\frac{\zeta^2p^2q^2z}{16\overline{\gamma_2}\alpha}\middle|\begin{matrix}1-n,\frac{\varphi^2+1}{2},\frac{\varphi^2+2}{2}\\ \frac{\varphi^2}{2},\frac{\varphi^2+1}{2},\frac{p}{2},\frac{p+1}{2},\frac{q}{2},\frac{q+1}{2}\end{matrix}\right]\quad(\beta>\alpha\rho)\tag{27}$$

where $A=\dfrac{\varphi^2 2^{p+q-1}}{4\pi\Gamma(p)\Gamma(q)}\dfrac{\beta^{N_rM_r}}{\Gamma(N_rM_r)}\exp((\rho+1)\alpha)$

4. Outage Probability Analysis

In this section, the analytical expressions of OP are derived using CDF-based method. Moreover, asymptotic expressions are provided to predict the diversity order of the system in this part.

4.1 Outage Probability

Generally, OP is defined as the probability that SNR or SINR falls below a certain threshold [17]. In this system, we discuss the OP performance for both RF/FSO (S1-R-S2) and FSO/RF (S2-R-S1) links, which can efficiently evaluate the performance of the two-way system.

For S1-R-S2 link, there is $\gamma_{SINR}^{S2} \leq \kappa\mu min(\gamma_2, \frac{\gamma_1}{\kappa\mu\gamma_R+1})$, OP can be expressed as

$$\begin{aligned} P_{OUT}^{S1-S2} &= Pr\left[\kappa\mu min\left(\gamma_2, \frac{\gamma_1}{\kappa\mu\gamma_R+1}\right) \leq \gamma_{th}\right] \\ &= 1 - Pr\left[\gamma_2 > \frac{\gamma_{th}}{\kappa\mu}\right] Pr\left[\frac{\gamma_1}{\kappa\mu\gamma_R+1} > \frac{\gamma_{th}}{\kappa\mu}\right] \\ &= F_{\gamma_2}\left(\frac{\gamma_{th}}{\kappa\mu}\right) + F_{\frac{\gamma_1}{\kappa\mu\gamma_R+1}}\left(\frac{\gamma_{th}}{\kappa\mu}\right) - F_{\gamma_2}\left(\frac{\gamma_{th}}{\kappa\mu}\right) F_{\frac{\gamma_1}{\kappa\mu\gamma_R+1}}\left(\frac{\gamma_{th}}{\kappa\mu}\right) \end{aligned} \tag{28}$$

All the CDFs mentioned in Eq. (28), have been derived above, substituting Eq. (17) and Eq. (21) into Eq. (28), the final OP for S1-R-S2 link is obtained.

Likewise, the same way is adopted for calculating OP for S2-R-S1 links, assumed $\frac{\gamma_1}{\gamma_S}$ and $\frac{\gamma_2}{\gamma_S+\rho\gamma_R}$ are independent, still $\gamma_{SINR}^{S1} \leq \rho min(\frac{\gamma_1}{\gamma_S}, \frac{\gamma_2}{\gamma_S+\rho\gamma_R})$, there is

$$P_{OUT}^{S2-S1} = F_{\frac{\gamma_1}{\gamma_S}}\left(\frac{\gamma_{th}}{\rho}\right) + F_{\frac{\gamma_2}{\gamma_S+\rho\gamma_R}}\left(\frac{\gamma_{th}}{\rho}\right) - F_{\frac{\gamma_1}{\gamma_S}}\left(\frac{\gamma_{th}}{\rho}\right) F_{\frac{\gamma_2}{\gamma_S+\rho\gamma_R}}\left(\frac{\gamma_{th}}{\rho}\right) \tag{29}$$

Using Eq. (20) and Eq. (27), the expression of OP for S2-R-S1 link is obtained.

4.2 Asymptotic Outage Probability

Since we have derived the exact OP expressions of the two-way system in the previous section, the asymptotic OP will be further discussed in this part to assess the system performance. Generally, asymptotic OP can be written by $P_{out}^{\infty} \simeq (G_c SNR)^{-G_d}$, where G_c denotes coding gain, G_d represents the diversity order of the system [18].

Useful approximations are listed as

$$\begin{aligned} exp(x) &= \sum_{i=0}^{k} \frac{x^i}{i!} + o(x^k) x \to 0 \\ 1 - \frac{\Gamma(m,x)}{\Gamma(m)} &= \frac{x^m}{\Gamma(m+1)} x \to 0 \end{aligned} \tag{30}$$

For S1-R-S2 link, the exact OP performance can be obtained by Eq. (28), which can be divided into three parts. However, for asymptotic OP analysis, the third part will be negligible, since high SNR lead to lower value of CDF, the multiplication of two CDFs will be especially small which can be removed. To simplify calculation, we set $\mu = \kappa = \rho = 1$ in the following derivation. Thus, according to Eq. (28), the asymptotic OP can be given as

$$P_{out,S1-S2}^{\infty} \simeq F_{\gamma_2}^{\infty}(\gamma_{th}) + F_{\gamma_1/(\gamma_R+1)}^{\infty}(\gamma_{th}) \tag{31}$$

where $F_{\gamma_2}^{\infty}(\gamma_{th})$ and $F_{\gamma_1/(\gamma_R+1)}^{\infty}(\gamma_{th})$ denote the CDFs of γ_2 and $\gamma_1/(\gamma_R+1)$ at high SNR, respectively.

As $\overline{\gamma} \to \infty$, there is $\gamma_{th}/\overline{\gamma} \to 0$, by using Eq. (30), asymptotic expression for Eq. (21) can be simplified to

$$F_{\frac{\gamma_1}{\gamma_R+1}}^{\infty}(\gamma_{th}) = \frac{(\beta)^{N_r M_r}}{\Gamma(N_r M_r)} \frac{(2a)^{m_1}}{\Gamma(m_1+1)} \sum_{l=0}^{m_1} \binom{m_1}{l} (2)^{-l} \frac{\Gamma(l+N_r M_r)}{\beta^{l+N_r M_r}} \left(\frac{\gamma_{th}}{\overline{\gamma_1}}\right)^{m_1} \tag{32}$$

Moreover, when $\gamma_{th}/\overline{\gamma} \to 0$, Meijer-G function in Eq. (17) has series representation based on [16, Eq. (07.34.06.0006.01)], the asymptotic expression is obtained as

$$F_{\gamma_2}^{\infty}(\gamma_{th}) = \Lambda_1 \sum_{k=1}^{6} \frac{\Pi_{j=1,j\neq k}^{6} \Gamma(b_j - b_k)}{\Pi_{j=2}^{3} \Gamma(a_j - b_k) b_k} \left(\frac{p^2 q^2 \zeta^2 \gamma_{th}}{16\overline{\gamma_2}}\right)^{b_k} \tag{33}$$

where $\Lambda_1 = \frac{2^{p+q-2}\varphi^2}{2\pi\Gamma(p)\Gamma(q)}$, $a_j = \{1, \frac{\varphi^2+1}{2}, \frac{\varphi^2+2}{2}\}$, $b_k = \{\frac{\varphi^2}{2}, \frac{\varphi^2+1}{2}, \frac{p}{2}, \frac{p+1}{2}, \frac{q}{2}, \frac{q+1}{2}\}$. The main value of Eq. (33) is determined by the items with smaller power. Hence, a simpler asymptotic

expression can be derived by only considering the minimum parameter b_k. Thus, the final expression is shown as

$$F_{\gamma_2}^{\infty}(\gamma_{th}) = \Lambda_1 \frac{\Pi_{j=1,b_j\neq\nu_1}^{6}\Gamma(b_j-\nu_1)}{\Pi_{j=2}^{3}\Gamma(a_j-\nu_1)\,\nu_1}\left(\frac{p^2q^2\zeta^2\gamma_{th}}{16\overline{\gamma_2}}\right)^{\nu_1} \tag{34}$$

where $\nu_1 = min(\frac{\varphi^2}{2}, \frac{p}{2}, \frac{q}{2})$.

Substituting Eq. (32) and Eq. (34) into Eq. (31), the asymptotic OP for S1-R-S2 link is given by

$$\begin{aligned} P_{out,S1-S2}^{\infty} \simeq\ & \Lambda_1 \frac{\Pi_{j=1,b_j\neq\nu_1}^{6}\Gamma(b_j-\nu_1)}{\Pi_{j=2}^{3}\Gamma(a_j-\nu_1)\,\nu_1}\left(\frac{p^2q^2\zeta^2\gamma_{th}}{16\overline{\gamma_2}}\right)^{\nu_1} \\ & + \frac{(\beta)^{N_rM_r}}{\Gamma(N_rM_r)}\frac{(2a)^{m_1}}{\Gamma(m_1+1)}\sum_{l=0}^{m_1}\binom{m_1}{l}(2)^{-l}\frac{\Gamma(l+N_rM_r)}{\beta^{l+N_rM_r}}\left(\frac{\gamma_{th}}{\overline{\gamma_1}}\right)^{m_1} \end{aligned} \tag{35}$$

The main value of Eq. (35) is determined by the items with smaller power. Hence, we can conclude that the diversity order of the system is presented as $d = \min\{m_1, \nu_1\}$.

Similarly, the derivation of asymptotic OP for S2-R-S1 link is shown as follows

$$P_{out,S2-S1}^{\infty} \simeq F_{\gamma_1/\gamma_S}^{\infty}(\gamma_{th}) + F_{\gamma_2/(\gamma_S+\gamma_R)}^{\infty}(\gamma_{th}) \tag{36}$$

where $F_{\gamma_1/\gamma_S}^{\infty}(\gamma_{th})$ and $F_{\gamma_2/(\gamma_S+\gamma_R)}^{\infty}(\gamma_{th})$ denote CDFs of γ_1/γ_S and $\gamma_2/(\gamma_S+\gamma_R)$ at high SNR, respectively.

As $\overline{\gamma}\to\infty$, $\gamma_{th}/\overline{\gamma}\to 0$, asymptotic expression for Eq. (20) can be simplified via Taylor's series

$$F_{\gamma_1/\gamma_S}^{\infty}(\gamma_{th}) = \frac{\alpha^{N_sm_s}}{\Gamma(N_sm_s)}\frac{a^{m_1}}{\Gamma(m_1+1)}\sum_{l=0}^{m_1}\binom{m_1}{l}\frac{\Gamma(l+N_sm_s)}{\alpha^{l+N_sm_s}}\left(\frac{\gamma_{th}}{\overline{\gamma_1}}\right)^{m_1} \tag{37}$$

Asymptotic expression for Eq. (27) needs the expansion of Meijer-G function as above, result can be approximated as

$$\begin{aligned} F_{\gamma_2/(\gamma_S+\gamma_R)}^{\infty}(\gamma_{th}) = A & \sum_{t=0}^{N_sM_s-1}\sum_{k=0}^{t}\sum_{n=0}^{t-k}\binom{t}{k}\binom{t-k}{n}\frac{\alpha^{t-n}(-1)^k}{t!}\frac{\Gamma(k+N_rM_r)}{(\beta-\alpha)^{k+N_rM_r}}(-2)^{t-k-n} \\ & \times\sum_{k=1}^{6}\frac{\Pi_{j=1,j\neq k}^{6}\Gamma(b_j-b_k)\,\Gamma(n+b_k)}{\Pi_{j=2}^{3}\Gamma(a_j-b_k)}\left(\frac{p^2q^2\zeta^2\gamma_{th}}{16\alpha\overline{\gamma_2}}\right)^{b_k}\ (\beta>\alpha) \end{aligned} \tag{38}$$

Result of Eq. (38) can be further simplified via only one dominant term. By substituting Eq. (37) and Eq. (38) into Eq. (36), the final asymptotic OP for S2-R-S1 link is given by

$$\begin{aligned} P_{out,S2-S1}^{\infty} \simeq\ & \frac{\alpha^{N_sm_s}}{\Gamma(N_sm_s)}\frac{a^{m_1}}{\Gamma(m_1+1)}\sum_{l=0}^{m_1}\binom{m_1}{l}\frac{\Gamma(l+N_sm_s)}{\alpha^{l+N_sm_s}}\left(\frac{\gamma_{th}}{\overline{\gamma_1}}\right)^{m_1} \\ & + A\sum_{t=0}^{N_sM_s-1}\sum_{k=0}^{t}\sum_{n=0}^{t-k}\binom{t}{k}\binom{t-k}{n}\frac{\alpha^{t-n}(-1)^k}{t!} \\ & \times\frac{\Gamma(k+N_rM_r)}{(\beta-\alpha)^{k+N_rM_r}}(-2)^{t-k-n}\frac{\Pi_{j=1,j\neq k}^{6}\Gamma(b_j-\nu_2)\,\Gamma(n+\nu_2)}{\Pi_{j=2}^{3}\Gamma(a_j-\nu_2)}\left(\frac{p^2q^2\zeta^2\gamma_{th}}{16\alpha\overline{\gamma_2}}\right)^{\nu_2}(\beta>\alpha) \end{aligned} \tag{39}$$

where $\nu_2 = min(\frac{\varphi^2}{2}, \frac{p}{2}, \frac{q}{2})$. The diversity order of the system can be expressed as $d = min\{m_1, \nu_2\}$.

5. BER and Outage Capacity Analysis

Since exact OP and asymptotic OP expressions have been derived in previous section, we further investigate BER and outage capacity performance in this section.

5.1 Bit Error Rate

BER expressions are derived based on CDFs method. In order to achieve a better BER performance, BPSK modulation is adopted instead of other modulation schemes. Thus, BER can be expressed as [19]

$$P_e = \frac{1}{2\sqrt{2\pi}} \int_0^\infty \frac{1}{\sqrt{x}} F_\gamma\left(\frac{x}{2}\right) \exp\left(-\frac{x}{2}\right) dx \tag{40}$$

Substituting Eq. (28) into Eq. (40), BER of S1-R-S2 link is obtained, and the calculation can be divided into three items as

$$\begin{aligned} P_e^{s_1-s_2} &= P_{e1}^{s_1-s_2} + P_{e2}^{s_1-s_2} - P_{e3}^{s_1-s_2} \\ &= \frac{1}{2\sqrt{2\pi}} \int_0^\infty \frac{\exp(-x/2)}{\sqrt{x}} F_{\gamma_2}\left(\frac{x}{2}\right) dx + \frac{1}{2\sqrt{2\pi}} \int_0^\infty \frac{\exp(-x/2)}{\sqrt{x}} \\ &\quad \times F_{\frac{\gamma_1}{\gamma_R+1}}\left(\frac{x}{2}\right) dx - \frac{1}{2\sqrt{2\pi}} \int_0^\infty \frac{\exp(-x/2)}{\sqrt{x}} F_{\gamma_2}\left(\frac{x}{2}\right) F_{\frac{\gamma_1}{\gamma_R+1}}\left(\frac{x}{2}\right) dx \end{aligned} \tag{41}$$

Substituting Eq. (17) into Eq. (41), using [16, Eq. (07.34.21.0013.01)] for integral, first block can be expressed as

$$P_{e1}^{s_1-s_2} = \frac{2^{p+q-4}\varphi^2}{\pi^{3/2}\Gamma(p)\Gamma(q)} G_{4,7}^{6,2}\left[\frac{p^2q^2\zeta^2}{16\overline{\gamma_2}}\middle| \begin{matrix} 1, 0.5, \frac{\varphi^2+1}{2}, \frac{\varphi^2+2}{2} \\ \frac{\varphi^2}{2}, \frac{\varphi^2+1}{2}, \frac{p}{2}, \frac{p+1}{2}, \frac{q}{2}, \frac{q+1}{2}, 0 \end{matrix}\right] \tag{42}$$

The same way is adopted to derive other items, after integral from three Meijer G functions using [20, Eq. (20)] and some mathematical simplifications, there are

$$\begin{aligned} P_{e2}^{s_1-s_2} &= \frac{1}{2} - \frac{1}{2\sqrt{2\pi}} \frac{\beta^{N_r m_r}}{\Gamma(N_r m_r)} \sum_{l=0}^{m_1-1} \sum_{d=0}^{l} \binom{l}{d} \left(\frac{a}{2\overline{\gamma_1}}\right)^l \\ &\quad \times \frac{(2)^{l-d}}{\beta^{d+N_r m_r} l!} \lambda_1^{-l-\frac{1}{2}} G_{2,1}^{1,2}\left[\frac{a}{2\beta\overline{\gamma_1}\lambda_1}\middle| \begin{matrix} \omega_1, \omega_2 \\ 0 \end{matrix}\right] \end{aligned} \tag{43}$$

$$\begin{aligned} P_{e3}^{s_1-s_2} &= P_{e1}^{s_1-s_2} - \frac{2^{p+q-4}\varphi^2}{\pi\sqrt{2\pi}\Gamma(p)\Gamma(q)} \frac{\beta^{N_r m_r}}{\Gamma(N_r m_r)} \sum_{l=0}^{m_1-1} \sum_{d=0}^{l} \binom{l}{d} \left(\frac{a}{2\overline{\gamma_1}}\right)^l \frac{(2)^{l-d}}{\beta^{d+N_r m_r} l!} \\ &\quad \lambda_1^{-(l+0.5)} G_{1,0;1,1;6,1}^{1,0;1,1;6,1}\left[\begin{matrix} \omega_1 \\ - \end{matrix}\middle| \begin{matrix} \omega_2 \\ 0 \end{matrix}\middle| \begin{matrix} \omega_3 \\ \omega_4 \end{matrix}\middle| \frac{a}{2\beta\overline{\gamma_1}\lambda_1}, \frac{p^2q^2\zeta^2}{32\overline{\gamma_2}\lambda_1}\right] \end{aligned} \tag{44}$$

where $\lambda_1 = \frac{1}{2} + \frac{a}{\overline{\gamma_1}}$ and $\{\omega_1, \omega_2, \omega_3, \omega_4\} = \{0.5 - l, 1 - d - N_r m_r, (1, \frac{\varphi^2+1}{2}, \frac{\varphi^2+2}{2}), (\frac{\varphi^2}{2}, \frac{\varphi^2+1}{2}, \frac{p}{2}, \frac{p+1}{2}, \frac{q}{2}, \frac{q+1}{2}, 0)\}$. $G_{\cdots;\cdots;\cdots;\cdots;\cdots;\cdots}^{\cdots;\cdots;\cdots}\left[\begin{matrix}..\\..\end{matrix}\middle|\begin{matrix}..\\..\end{matrix}\middle|\begin{matrix}..\\..\end{matrix}\middle|\ldots, \ldots\right]$ is the extended generalized bivariate Meijer G-function (EGBMGF). An efficient MATHEMATICA implementation of the EGBMGF is given in [20].

Similarly, BER for S2-R-S1 link can also be calculated by repeating the above process, expressions for three items can be given as

$$P_{e4}^{S_2-S_1} = \frac{1}{2} - \frac{1}{2\sqrt{2\pi}} \frac{\alpha^{N_s m_s}}{\Gamma(N_s m_s)} \sum_{i=0}^{m_1-1} \sum_{j=0}^{i} \binom{i}{j} \left(\frac{a}{2\sqrt{\gamma_1}}\right)^i \frac{\alpha^{-(j+N_s m_s)}}{i!} \lambda_2{}^{-i-0.5} G_{2,1}^{1,2}\left[\frac{a}{2\alpha\sqrt{\gamma_1}\lambda_2} \middle| \begin{matrix}\omega_5, 0.5-i \\ 0\end{matrix}\right] \tag{45}$$

$$P_{e5}^{S_2-S_1} = B \sum_{t=0}^{N_s M_s-1} \sum_{k=0}^{t} \sum_{n=0}^{t-k} \binom{t}{k} \binom{t-k}{n} \frac{\alpha^{t-n}(-1)^k}{t!} \frac{\Gamma(k+N_r M_r)}{(\beta-\alpha)^{k+N_r M_r}} (-2)^{t-k-n} \times G_{4,6}^{6,2}\left[\frac{p^2 q^2 \zeta^2}{16\alpha\sqrt{\gamma_2}} \middle| \begin{matrix}\omega_6, 0.5 \\ \omega_7\end{matrix}\right] \quad (\beta > \alpha\rho) \tag{46}$$

$$P_{e6}^{S_2-S_1} = P_{e5}^{S_2-S_1} - B \frac{\alpha^{N_s m_s}}{\Gamma(N_s m_s)} \sum_{t=0}^{N_s M_s-1} \sum_{k=0}^{t} \binom{t}{k} \sum_{n=0}^{t-k} \binom{t-k}{n} \frac{\alpha^{t-n}(-1)^k}{t!} \times \frac{\Gamma(k+N_r M_r)}{(\beta-\alpha)^{k+N_r M_r}} (-2)^{t-k-n} \sum_{i=0}^{m_1-1} \sum_{j=0}^{i} \binom{i}{j} \left(\frac{a}{2\sqrt{\gamma_1}}\right)^i \frac{\alpha^{-(j+N_s m_s)}}{i!} \lambda_2{}^{-(i+0.5)} \times G_{1,0;1,1;6,1}^{1,0;1,1;3,6}\left[\begin{matrix}0.5-i \\ -\end{matrix} \middle| \begin{matrix}\omega_5 \\ 0\end{matrix} \middle| \begin{matrix}\omega_6 \\ \omega_7\end{matrix} \middle| \frac{a}{2\alpha\sqrt{\gamma_1}\lambda_2}, \frac{p^2 q^2 \zeta^2}{32\alpha\sqrt{\gamma_2}\lambda_2}\right] \tag{47}$$

where $\lambda_2 = \frac{1}{2} + \frac{a}{2\sqrt{\gamma_1}}$ and $\{\omega_5, \omega_6, \omega_7\} = \left\{1-j-N_S m_S, \left(1-n, \frac{\varphi^2+1}{2}, \frac{\varphi^2+2}{2}\right), \left(\frac{\varphi^2}{2}, \frac{\varphi^2+1}{2}, \frac{p}{2}, \frac{p+1}{2}, \frac{q}{2}, \frac{q+1}{2}\right)\right\}$. $B = \frac{2^{p+q-4}\varphi^2 \beta^{N_r M_r} \exp(2\alpha)}{\pi\sqrt{\pi}\Gamma(p)\Gamma(q)\Gamma(N_r M_r)}$. $P_e^{S_2-S_1}$ is the sum of the three items above, which can be easily expressed.

5.2 Outage Capacity

Outage capacity is another important metric to describe the average throughput of the system. Generally, Outage capacity is defined as the probability that the throughput falls below a predetermined threshold C_T as follows [11]

$$R(C_T) = \Pr(\overline{C} \le C_T) = F_\gamma(2^{C_T} - 1) \tag{48}$$

By substituting Eq. (28) and Eq. (29) into Eq. (48), final results can be obtained.

6. Simulation Results

In this section, the numerical results of OP, BER and outage capacity based on two-way mixed RF/FSO are demonstrated and verified by simulations. Additionally, the effect of various parameters on system performance such as interference numbers and power are investigated and compared including interference-free condition. To simplify simulations, we assume all CCIs follow i.i.d. and $m_1 = m_s = m_r = 2$, $\Omega_1 = \Omega_s = \Omega_r = 1$, $\rho = \kappa = \mu = 1$.

Fig. 2 demonstrates the OP performance of RF-FSO link over different interference numbers and power when CCIs are only considered at relay. The curves are plotted as a function of average SNR over FSO links, and system parameters are set as p = 2.902, q = 2.51, γth = 7dB, $\overline{\gamma_1}$ = 40dB. It can be noted from the figure, for interference-effected system, when average SNR over FSO links increases, OP decreases first and then becomes stable. These outage floors cannot be decreased by further increasing average SNR over FSO links, which implies RF link becomes dominant and its performance is limited by interference. However, for interference-free system, this phenomenon does not exist. As expected, OP increases as the numbers and power of interference increases. Moreover, it finds that as the interference power increased, the effect of interference numbers becomes severer.

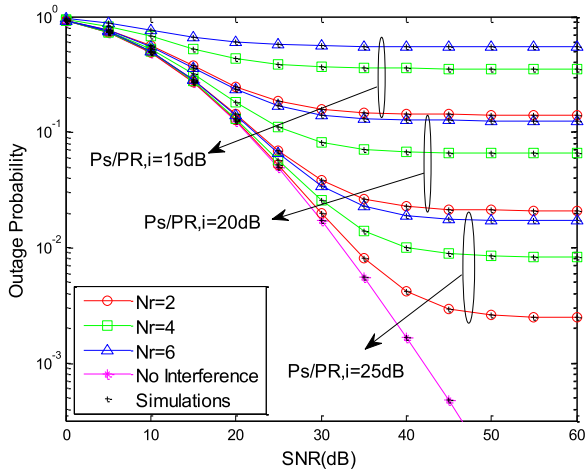

Fig. 2. OP of RF-FSO link over different interference numbers and power based on average SNR over FSO links.

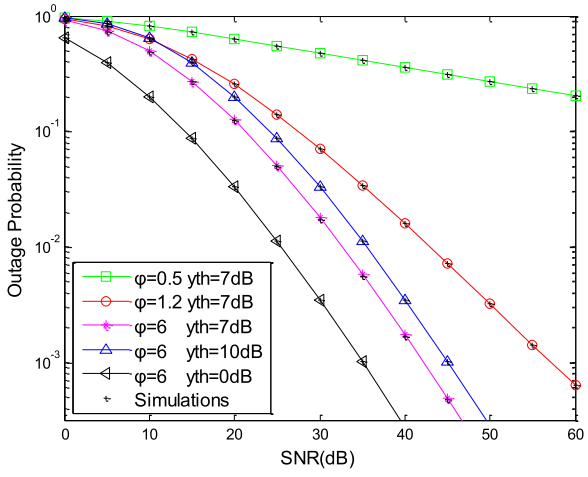

Fig. 3. OP of RF-FSO link over different values of φ and γth based on average SNR over FSO links.

Fig. 3 illustrates the OP of RF-FSO link with different value of φ and γth in interference-free case. As observed, for strong pointing errors case (small φ), the OP performance is seriously affected. However, when φ increases, the OP performance is enhanced. Additionally, OP performance is improved as γth decreases.

Fig. 4 presents the OP performance of FSO-RF link with different interference numbers and power when the CCIs are considered at both relay and S1. In order to further explore the effect of CCIs at S1 on OP performance, the CCIs at relay are fixed as Nr $= 1$, Ps/$P_{R,i} = 40$ dB. As observed, outage floor appears when average SNR increases. In addition, OP performance decreases when the numbers and power of interference increase, as the power of interference get larger, the effect of interference number on OP become more serious.

Fig. 5 compares the OP performance of two-way mixed RF/FSO system in the presence of CCIs based on average SNR over FSO links. It can be noted from the figure, the asymptotic OP is consistent with the exact OP when SNR is high, which implies the accuracy of asymptotic expressions. Moreover, when interference is only considered at relay, the OP performance of RF-FSO and FSO-RF links is nearly the same. However, when the interference at S1 cannot be ignored, the performance of the RF-FSO link is far better than that of FSO-RF link.

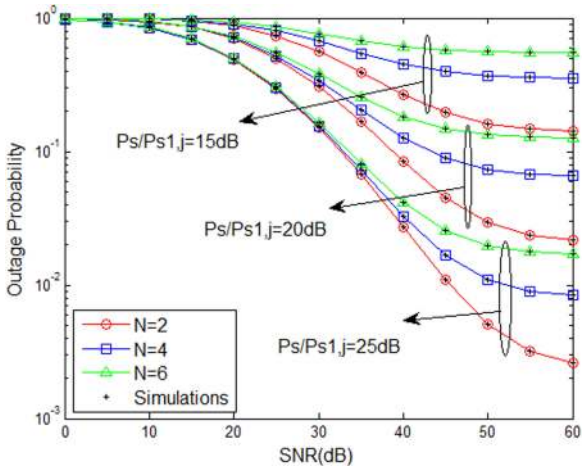

Fig. 4. OP of FSO-RF link over different interference numbers and power based on average SNR over FSO links.

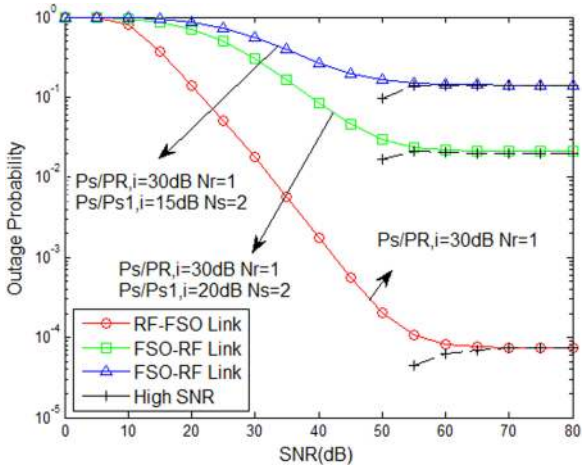

Fig. 5. OP of two-way links over different interference numbers and power based on average SNR over FSO links.

To further investigate and verify the effect of CCIs on system performance, BERs of the two-way mixed RF/FSO system are simulated and discussed. Fig. 6 and Fig. 7 plot BERs of RF-FSO and FSO-RF links versus average SNR over FSO links, respectively. In Fig. 6, the BER floor does not exist for interference-free condition. However, for interference-effected case, it is obvious that with the increment of interference power and numbers, BER performance decreases dramatically. In Fig. 7, we fix the CCIs at relay as Nr $=$ 1, Ps/$P_{R,j}$ $=$ 40 dB to further investigate the effect of interference at S1 on BER performance. Similar observations can be made as Fig. 6, BER floors occur in all interference-effected cases. Moreover, it can be noted that when interference power is small, BERs have little gap for different interference numbers, it concludes that the effect of interference numbers on system performance is related to interference power.

Besides OP and BER, outage capacity is another important parameter to measure the average throughput of the system. Fig. 8 and Fig. 9 investigate the effect of threshold C_T and CCIs on outage capacity performance. It is obvious that, the lower threshold can achieve better throughput coverage. When threshold increases, the throughput quickly saturates and reaches the bottleneck. Moreover, in Fig. 9, system parameters are set as $C_T = 5$ dB. As expected, interference limits the

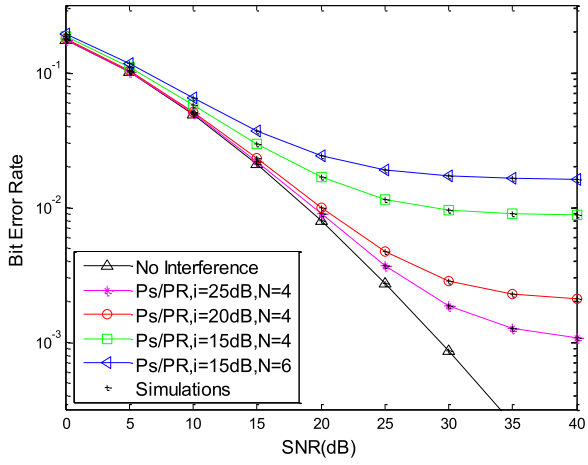

Fig. 6. BER of RF-FSO link over different interference numbers and power based on average SNR over FSO links.

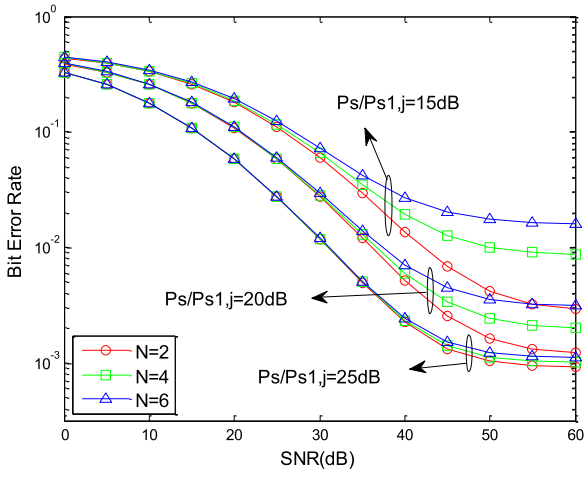

Fig. 7. BER of FSO-RF link over different interference numbers and power based on average SNR over FSO links.

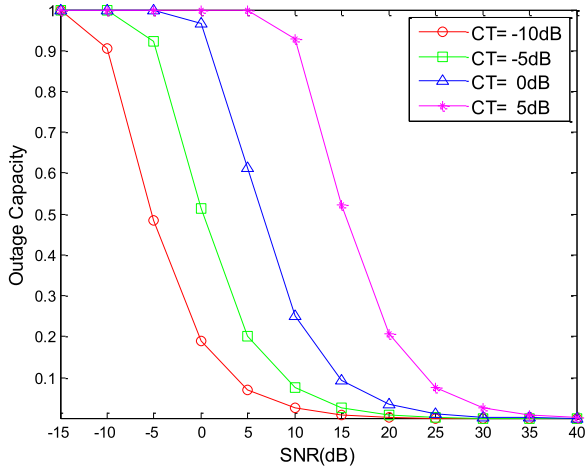

Fig. 8. Outage Capacity of RF-FSO link over different values of C_T based on average SNR over FSO links.

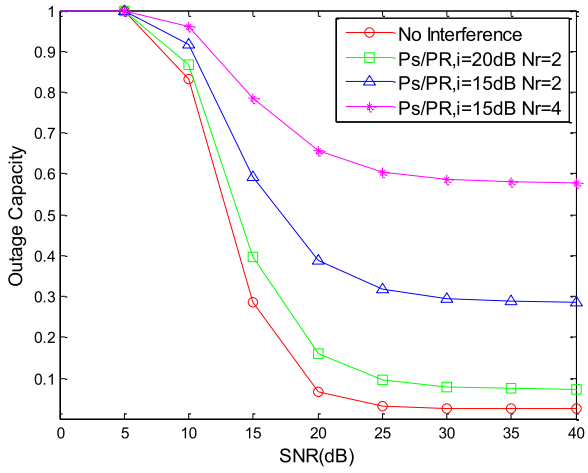

Fig. 9. Outage Capacity of RF-FSO link over different interference numbers and power based on average SNR over FSO links.

performance of outage capacity. Most importantly, in interference-effected system, outage capacity reaches the bottleneck and cannot be decreased by further increasing average SNR.

7. Conclusion

In this paper, the performance of a two-way mixed RF/FSO relaying system is investigated, and CCIs are considered at both relay and destination. The RF links follow Nakagami-m distribution, while FSO links adopt Gamma-Gamma turbulence model with pointing errors. Closed-form lower bounds expressions for OP, BER and outage capacity are derived and simulated for both RF/FSO and FSO/RF links. Asymptotic expressions are further provided to predict the diversity order. Additionally, the effect of various parameters on system performance is investigated and compared. Results demonstrate that system performance decreases as the numbers and power of interference increases, when the interference power increases, the effect of interference number becomes severer. Moreover, outage floor exists in interference-effected system, which implies RF link becomes dominant and its performance is limited by CCIs. This shows that to better reflect practical scenes, CCIs are quite important factor which cannot be ignored in system design.

References

[1] E. Balti, M. Guizani, B. Hamdaoui, and B. Khalfi, "Aggregate hardware impairments over mixed RF/FSO relaying systems with outdated CSI," *IEEE Trans. Commun.*, vol. 66, no. 3, pp. 1110–1122, Mar. 2018.
[2] M. A. Khalighi and M. Uysal, "Survey on free space optical communication: A communication theory perspective," *IEEE Commun. Surveys Tut.*, vol. 16, no. 4, pp. 2231–2258, Oct.–Dec. 2014.
[3] Y. F. Al-Eryani, A. M. Salhab, S. A. Zummo, and M.-S. Alouini, "Two-way multiuser mixed RF/FSO relaying: Performance analysis and power allocation," *IEEE/OSA J. Opt. Commun. Netw.*, vol. 10, no. 4, pp. 396–408, Apr. 2018.
[4] Y. F. Aleryani, A. M. Salhab, S. A. Zummo, and M.-S. Alouini, "On the performance of two-way multiuser mixed RF/FSO relay networks with opportunistic scheduling & asymmetric channel gains," in *Proc. IEEE Int. Wireless Commun. Mobile Comput. Conf.*, 2017, pp. 1178–1183.
[5] N. Sharma, P. Garg, and A. Bansal, "Mixed RF/FSO bidirectional system achieving spectral efficiency," *Photon. Netw. Commun.*, vol. 34, no. 1, pp. 93–99, 2017.
[6] T. V. Nguyen, T. V. M. Pham, T. A. Pham, H. T. T. Pham, N. T. Dang, and A. T. Pham, "Performance analysis of network-coded two-way dual-hop mixed FSO/RF systems," in *Proc. IEEE Int. Conf. Adv. Technol. Commun.*, 2017, pp. 70–75.
[7] L. Kong, W. Xu, H. Zhang, and C. Zhao, "Mixed RF/FSO two-way relaying system under generalized FSO channel with pointing error," in *Proc. 8th Int. Conf. Ubiquitous Future Netw.*, 2016, pp. 264–269.
[8] M. I. Petkovic, "Performance analysis of mixed RF/FSO systems," in *Proc. Telecommun. Forum Telfor*, 2015, pp. 293–300.

[9] M. I. Petkovic, A. M. Cvetkovic, G. T. Djordjevic, and G. K. Karagiannidis, "Outage performance of the mixed RF/FSO relaying channel in the presence of interference," *Wireless Pers. Commun.*, vol. 96, no. 21, pp. 1–16, 2017.
[10] E. Soleimani-Nasab and M. Uysal, "Generalized performance analysis of mixed RF/FSO cooperative systems," *IEEE Trans. Wireless Commun.*, vol. 15, no. 1, pp. 714–727, Jan. 2016.
[11] E. Balti and M. Guizani, "Mixed RF/FSO cooperative relaying systems with co-channel interference," *IEEE Trans. Commun.*, vol. 66, no. 9, pp. 4014–4027, Sep. 2018.
[12] A. H. A. El-Malek, A. M. Salhab, S. A. Zummo, and M.-S. Alouini, "Effect of RF interference on the security-reliability tradeoff analysis of multiuser mixed RF/FSO relay networks with power allocation," *J. Lightw. Technol.*, vol. 35, no. 9, pp. 1490–1505, May 2017.
[13] E. Soleimani-Nasab, M. Matthaiou, M. Ardebilipour, and G. K. Karagiannidis, "Two-way AF relaying in the presence of co-channel interference," *IEEE Trans. Commun.*, vol. 61, no. 8, pp. 3156–3169, Aug. 2013.
[14] A Touati, A. Abdaoui, F. Touati, M. Uysal, and A. Boullegue, "On the effects of combined atmospheric fading and misalignment on the hybrid FSO/RF transmission," *IEEE/OSA J. Opt. Commun. Netw.*, vol. 8, no. 10, pp. 715–725, Oct. 2016.
[15] I. S. Gradshteyn and I. M. Ryzhik, *Table of Integrals, Series and Products*, 6th ed. San Diego, CA, USA: Academic, 2000.
[16] The Wolfram Functions Site, 2015. Available at: http://functions.wolfram.com/HypergeometricFunctions/MeijerG/
[17] F. Al-Qahtani, A. A. El-Malek, I. Ansari, R. Radaydeh, and S. A. Zummo, "Outage analysis of mixed underlay cognitive RF MIMO and FSO relaying with interference reduction," *IEEE Photon. J.*, vol. 9, no. 2, pp. 1–22, Apr. 2017.
[18] M. K. Simon and M.-S. Alouini, *Digital Communication Over Fading Channels*, 2nd ed. Hoboken, NJ, USA: Wiley, 2005
[19] J. Park, E. Lee, G. Park, B. Roh, and G. Yoon, "Performance analysis of asymmetric RF/FSO dual-hop relaying systems for UAV applications," in *Proc. Military Commun. Conf.*, 2013, pp. 1651–1656.
[20] I. S. Ansari, S. Al-Ahmadi, F. Yilmaz, M.-S. Alouini, and H. Yanikomeroglu, "A new formula for the BER of binary modulations with dual-branch selection over generalized-k composite fading channels," *IEEE Trans. Commun.*, vol. 59, no. 10, pp. 2654–2658, Oct. 2011.